

AD-A229 357

REF ID: A229

(2)

OFFICE OF NAVAL RESEARCH

PUBLICATIONS/PATENTS/PRESENTATIONS/HONORS REPORT

for

October 1, 1989 through September 30, 1990

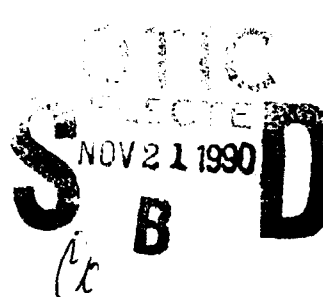
for

Contract N00014-87-K-0243

R&T #414e340

Materials Processing of Diamond:
Etching, Doping by Ion Implantation and Contact Formation

Max L. Swanson
University of North Carolina
Department of Physics and Astronomy
CB#3255 Phillips Hall
Chapel Hill, NC 27599-3255



Reproduction in whole, or in part, is permitted for any purpose of the United States Government.

This document has been approved for public release and sale; its distribution is unlimited.

100-210-014

a. Papers submitted and not yet published

"Annealing of Implantation Damage in Single Crystal Diamond," J.D. Hunn, M.L. Swanson, E.A. Hill, N.R. Parikh, and G. Hudson , Second International Conference on New Diamond Science and Technology, Washington, DC, September 23-27, 1990.

b. Papers published and accepted for publication

1. "Regrowth of Radiation-Damaged Layers in Natural Diamond," B. Liu, G.S. Sandhu, N.R. Parikh, and M.L. Swanson, Nucl. Instr. Meth. B45, 420 (1990).
2. "Regrowth of Damaged Layers in Diamond Produced by Ion Implantation," G.S. Sandhu, B. Liu, N.R. Parikh, J.D. Hunn, M.L. Swanson, Th. Wichert, M. Deicher, H. Skudlik, W.N. Lennard, and I.V. Mitchell, Mat. Res. Soc. Symp. Proc. 162, 189 (1990).
3. "Doping of Diamond by Co-Implantation with Dopant Atoms and Carbon," G.S. Sandhu, C.T. Kao, M.L. Swanson, and W.K. Chu, Mat. Res. Soc. Symp. Proc. 162, 321 (1990).
4. "Annealing of Implantation Damage in Single Crystal Diamond," J.D. Hunn, M.L. Swanson, E.A. Hill, N.R. Parikh, and G. Hudson, Second International Conference on New Diamond Science and Technology, Washington, DC, September 23-27, 1990; to be published by MRS.
5. "Epitaxial Growth of Cu-Ni Single Alloys and Multilayers by Molecular Beam Epitaxy," R.P. Burns, Y.H. Lee, N.R. Parikh, J.B. Posthill, M.J. Mantini, and R.J. Markunas, Symp. D, MRS Fall 1989, Boston, MA., November 27 - December 2, 1989.

c. Books submitted for publication

none

d. Books published

none

e. Patent filed

none

f. Patents granted

none

g. Invited presentations

none

Acceptance For	
NTIS	<input checked="" type="checkbox"/>
DOE	<input type="checkbox"/>
Other	<input type="checkbox"/>
Distribution	
By	
Distribution/	
Availability Codes	
Dist	Avail. And/or special
A-1	

h. Contributed presentations

"Regrowth of Damaged Layers in Diamond Produced by Ion Implantation," G.S. Sandhu, B. Liu, N.R. Parikh, J.D. Hunn, M.L. Swanson, Th. Wichert, M. Deicher, H. Skudlik, W.N. Lennard, and I.V. Mitchell, MRS Fall Meeting 1989, Boston, MA., Symp.F, November 28 - December 1, 1989.

"Doping of Diamond by Co-Implantation with Dopant Atoms and Carbon," G.S. Sandhu, C.T. Kao, M.L. Swanson, and W.K. Chu, MRS Fall Meeting 1989, Boston, MA., Symp. F, November 27 - December 2, 1989.

"Thermal Annealing of Damage Caused by Carbon Implantation in Type I-a Diamond," J.D. Hunn, E.A. Hill, M.L. Swanson, and N.R. Parikh, Second International Conference on New Diamond Science and Technology (ICNDST-2), Washington, DC, September 23-27, 1990.

"Implantation Doping of Diamond," E.A. Hill, N.R. Parikh, J.D. Hunn, M.L. Swanson, R.A. Zuh, IBMM, Knoxville, TN., September 9-14, 1990.

"Epitaxial Growth of Cu-Ni Single Alloys and Multilayers by Molecular Beam Epitaxy," R.P. Burns, Y.H. Lee, N.R. Parikh, J.B. Posthill, M.J. Mantini, and R.J. Markunas, Symp. D, MRS Fall 1989, Boston, MA., November 27 - December 2, 1989.

i. Honors, awards, prizes

none

j. Graduate students and post-doctorals supported

Graduate students: G.S. Sandhu
J.D. Hunn
E.A. Hill

OFFICE OF NAVAL RESEARCH

1 October 1989 through 30 September 1990

Contract N00014-87-K-0243

R&T No 414e340

ANNUAL TECHNICAL REPORT

Materials Processing of Diamond:
Etching, Doping by Ion Implantation and Contact Formation

Max L. Swanson, Principal Investigator
Department of Physics and Astronomy
University of North Carolina
Chapel Hill, NC 27599-3255

(919) 962-0305

Reproduction in whole, or in part, is permitted for any purpose of the United States Government.

This document has been approved for public release and sale; its distribution is unlimited.

I. OVERVIEW

We are studying contact formation, regrowth and implantation doping of natural diamond, for future applications to the fabrication of devices from thin film CVD diamond. In addition, we are characterizing thin film diamonds of other ONR contractors, using ion beam methods.

In the last year, we have concentrated on the regrowth of ion damaged layers of diamond and the doping of diamond by implantation with Na, Li and F. We observed that complete regrowth of C ion damaged diamond occurred below a critical ion dose. Above that dose, a "green phase" occurred, which was characterized by a golden green color and by the absence of recovery of the lattice, as measured by ion channeling. Implantation doping studies of Li, Na, and F were initiated, and show some promise for n-type doping of diamond. The diffusivity of Li in diamond was studied by neutron depth profiling.

II. RESULTS

1. Regrowth

In previous results,^{1,2} we have reported that epitaxial regrowth of ion damaged diamond occurred during annealing at 900°C, even when the damaged level had reached a completely randomized state, as observed by ion channeling. However, a thin graphite layer of about 50 nm was formed on the surface during the annealing, which was in a vacuum of $\sim 10^{-6}$ torr. We have now completed a careful series of experiments in natural type I a and II a diamonds, that were damaged to different C ion doses, and annealed both in vacuum and by rapid thermal annealing (RTA) in argon. Since we did not observe graphite formation in any of these experiments, we conclude that the previous thin graphite layer was due to oxygen contamination during the annealing.

The present results³ show that the damage produced at 77 K by doses of less than 1.5×10^{15} C ions/cm² at 100 keV annealed out completely at 900°C as observed by ion channeling. This epitaxial regrowth of "randomized" diamond occurred for damaged layers at various depths below the surface.

Above this critical dose, the ion channeling damage showed no recovery at all, and the diamond became a golden green color. This "green phase" may represent a new form of diamond. Although radiation coloration is well known in the literature, no evidence for a stable, radiation-induced phase has been reported. It is possible that this phase represents an ordered structure of vacancy clusters in the diamond, similar to ordered void structures in metals.

This work is attached as appendices A and B.

2. Doping

A complete account of the doping experiments, as well as the regrowth and etching results up to the end of 1989, is presented in the Ph.D. thesis of G.S. Sandhu.⁴ It was concluded that the dual doping of C + B at 77 K was an effective way of introducing electrically active B into natural diamond. In addition, dual doping of C + N and C + P showed promising results for n-type doping. This work is continuing.

We have also started an implantation doping program, utilizing the group I dopants Li and Na, in collaboration with Oak Ridge National Laboratory. These elements have good possibilities⁵ as n-type dopants, according to theoretical studies. ²³Na and ⁶Li ions were implanted at 77 K into natural type II-a diamond to a dose of $10^{15}/\text{cm}^2$ with energies of 100 keV and 35 keV respectively.

Preliminary electrical measurements before and after annealing at 950°C indicated considerable electrical activation of the Na dopant. Neutron depth profiling, which is a very accurate method of measuring diffusivities of certain elements, was used to measure the concentration-depth profiles of the implanted ${}^6\text{Li}$ before and after annealing at 1000°C for 10 s. The annealing did not cause a measurable diffusion of the implanted Li.

These results are summarized in Appendices C and D.

3. Characterization

Sodium-doped thin films of diamond, grown by CVD at the Research Triangle Institute (RTI) have been examined by RBS. In some cases, a very high Na content was attained for these films.

The quality of epitaxial films of Cu-Ni grown at RTI by molecular beam epitaxy on Ni substrates, were studied by RBS/channeling. In the case of a 100 nm layer of Ni grown at 300°C, the normalized channeling yield was 7%, indicating a very good quality film.⁶

4. Contact Formation

Research to develop diamond contacts is continuing. The patent application for our sputtering method for Au contacts is still pending. Both B implantation and laser heating have been used for electrical contacts in our implantation doping experiments.

III. CONCLUSIONS

In the important area of the regrowth of ion damaged diamond, we have observed that a completely randomized lattice can be regrown when the damage level is below a certain threshold value, characterized by a deposited energy equivalent to 12 Frenkel defects per nm³, or about 7% defects. The kinetic mechanisms for regrowth under these conditions, and the influence of impurities such as F and H on the regrowth, are relevant to CVD growth.

A further interesting observation in the area of diamond defect structures was the occurrence of a radiation-induced "green phase", which occurred after annealing of samples that had been damaged above the threshold limit of 7% defects. This "phase" merits further investigation via Raman scattering, photoluminescence, etc.

A related diamond growth process that we plan to investigate is the epitaxial formation of diamond, which has been reported⁷ to occur during C ion implantation of Cu at elevated temperatures.

IV. REFERENCES

1. "Regrowth of Radiation-Damaged Layers in Natural Diamond," B. Liu, G.S. Sandhu, N.R. Parikh, and M.L. Swanson, Nucl. Instr. Meth. B45, 420 (1990).
2. "Regrowth of Damaged Layers in Diamond Produced by Ion Implantation," G.S. Sandhu, B. Liu, N.R. Parikh, J.D. Hunn, M.L. Swanson, Th. Wichert, M. Deicher, H. Skudlik, W.N. Lennard, and I.V. Mitchell, Mat. Res. Soc. Symp. Proc. 162, 189 (1990).
3. "Annealing of Implantation Damage in Single Crystal Diamond," J.D. Hunn, M.L. Swanson, E.A. Hill, N.R. Parikh, and G. Hudson, Second International Conference on New Diamond Science and Technology, Washington, DC, September 23-27, 1990, to be published by MRS.
4. G.S. Sandhu, Ph.D. thesis, Department of Physics and Astronomy, UNC-Chapel Hill, 1989.
5. "N-Type Doping and Donor Incorporation in Diamond," J. Bernholc, S. Kajihara, and A. Antonelli, Second International Conference on New Diamond Science and Technology, Washington, DC, September 23-27, 1990.
6. "Epitaxial Growth of Cu-Ni Single Alloys and Multilayers by Molecular Beam Epitaxy," R.P. Burns, Y.H. Lee, N.R. Parikh, J.B. Posthill, M.J. Mantini, and R.J. Markunas, Symp. D, MRS Fall 1989, Boston, MA., November 27 - December 2, 1989.
7. "A TEM Study of Layers Grown on Copper Using Carbon-ion Implantation," J.F. Prins and H.L. Gaigher, ICNDST-2, Washington, DC, September 23-27, 1990.

V. APPENDICES (attached)

- A. "Regrowth of Damaged Layers in Diamond Produced by Ion Implantation," G.S. Sandhu, B. Liu, N.R. Parikh, J.D. Hunn, M.L. Swanson, Th. Wichert, M. Deicher, H. Skudlik, W.N. Lennard, and I.V. Mitchell, Mat. Res. Soc. Symp. Proc. 162, 189 (1990).
- B. "Annealing of Implantation Damage in Single Crystal Diamond," J.D. Hunn, M.L. Swanson, E.A. Hill, N.R. Parikh, and G. Hudson, Second International Conference on New Diamond Science and Technology, Washington, DC, September 23-27, 1990, to be published by MRS.
- C. "Doping of Diamond by Co-Implantation with Dopant Atoms and Carbon," G.S. Sandhu, C.T. Kao, M.L. Swanson, and W.K. Chu, Mat. Res. Soc. Symp. Proc. 162, 321 (1990).
- D. "Ion Implantation Doping of Diamond," E. Hill, J. Hunn, N.R. Parikh, and M.L. Swanson, unpublished summary.
- E. "Impact of UNC-CH (Physics) Collaboration on RTI's Diamond Program," J.B. Posthill, October 16, 1989.

Annual Technical Reports Distribution List
 SDIO/IST Crystalline Carbon Materials Program
 (to be incorporated into report as its final pages)

<u>addressee</u>	<u>quantity</u>	<u>addressee</u>	<u>quantity</u>
1. ONR Arlington, VA 22217 ATTN: Code 1114 Code 1131M	8	2. Dr. M. Geis M.I.T. Lincoln Labs Lexington, MA 02173-0073	1
2. Defense Documentation Center Bldg. 5. Cameron Station Alexandria, VA 22314	12	3. Prof. R. Messier 265 Materials Res. Lab. University Park, PA 16802	1
3. Naval Research Laboratory Washington, DC 20375 ATTN: Code 4683 Code 2627 Code 6820 Code 6211 Code 6684 Code 6115 Code 4684 Code 6174	1 6 1 1 1 1 1 1	4. Prof. R. Davis Materials Eng., N.C.S.U. Raleigh, NC 27695-7907	1
4. Naval Ocean Systems Center San Diego, CA 92152 ATTN: Code 1211 Code 911 Code 56	1 1 1	5. R. Markunas R.T. Instit., P.O. Box 13164 R.T. Park, NC 27709-2164	1
5. (Co-chaired ONR Resident Representative or DCASMR)	1	6. Prof. G. Walrafen Howard Univ., Chemistry Dept. 5325 Potomac Ave., N.W. Washington, DC 20016	1
6. SDIO/IST Pentagon Washington, DC 20301-7100	1	7. Prof. I. Lindau Synchrotron Radiation Lab. Stanford, CA 94305	1
7. DAPPA/D.S.O. 1400 Wilson Blvd. Arlington, VA 22209	1	8. A. J. Purdes M.S. 147 Texas Instruments, P.O. Box 655936 Dallas, TX 75266	1
		9. W. D. Partlow Westinghouse R&D Ctr. 1310 Beulah Road Pittsburgh, PA 15235	1
		10. R. L. Adams 21002 N. 19th Ave., Suite 3 Phoenix, AZ 85021	1

Annual Technical Reports Distribution List
 SDIO/IST Crystalline Carbon Materials Program
 (to be incorporated into report as its final pages)

<u>addressee</u>	<u>quantity</u>	<u>addressee</u>	<u>quantity</u>
17. Prof. J. Angus Dept. of Chemistry Case Western Reserve Univ. Cleveland, OH 44106	1	27. Ken Hsu, Div 8347 Box 969 Sandia National Labs Livermore, CA 94550	1
18. T.R. Anthony, GE R&D Bldg. K-1, Room 1C30 Schenectady, NY 12345	1	28. Prof. W. Lanford Physics Dept. S.U.N.Y. Albany, NY 12222	1
19. Yehuda Arie SRI Sarnoff Center Princeton, NJ 08540	1	29. Prof. E.S. Machlin 44 Morningstar Drive Croton-on-Hudson, NY 10520	1
20. P.J. Boudreaux, Lab for Phys. Sci. 4928 College Avenue College Park, MD 20740	1	30. Prof. J. Mayer 210 Bard Hall Cornell University Ithaca, NY 14853	1
21. Prof. R.F. Bunshaw, UCLA 6532 Bueller Hall Los Angeles, CA 90024	1	31. Prof. J. Pancove, ECE Univ. of Colorado Boulder, CO 80309-0425	1
22. Ray Calloway, Aerospace Corp. P.O. Box 92957 Los Angeles, CA 90009	1	32. Michael Pinneo, Crystallume 3180 Porter Drive, Suite 2 Palo Alto, CA 94304	1
23. Prof. M.L. Swanson Phillips Hall CB# 3255 Chapel Hill, NC 27599-3255	1	33. Kenneth Russell J.P.L. M.S. 122-123 4800 Oak Grove Drive Pasadena, CA 91109	1
24. IBM T.J. Watson Center Yorktown Heights, NY 10598 ATTN: J.J. Cuomo B. Meyerson	1	34. Prof. T. D. Moustakas Exxon Research Annandale, NJ 08801	1
25. Prof. J. L. Davidson 200 Brown Hall Auburn Univ., AL 36849	1		
26. Prof. F.H. Fang, Dept. of Physics Boston College Chestnut Hill, MA 02167	1		

Enci. (2)

REGROWTH OF DAMAGED LAYERS IN DIAMOND PRODUCED BY ION IMPLANTATION

G.S. Sandhu, B. Liu, N.R. Parikh, J.D. Hunn, and M.L. Swanson, Department of Physics and Astronomy, University of North Carolina, Chapel Hill, NC 27599-3255; Th. Wichert, M. Deicher and H. Skudlik, University of Konstanz, Konstanz, FRG; and W.N. Lennard and I.V. Mitchell, University of Western Ontario, London, Ontario, Canada.

Abstract

We have used RBS/Channeling, perturbed angular correlation (PAC) and optical absorption to study the regrowth of disordered layers in diamond produced by implantation with carbon, or with carbon plus boron or indium ions. For C or C plus B implantation doses of $2 \times 10^{15} \text{ cm}^{-2}$ or less, complete recovery of channeling damage occurred after RTA at 1100°C or furnace annealing at 900°C. Optical measurements on samples implanted with high energy carbon ions show better recovery compared to the shallower implantations. PAC results showed that co-implantation with C and In caused a considerable fraction (~15%) of the In atoms to occupy well-defined lattice sites characterized by an electric field gradient having its major component along <111>, and a frequency of 116 MHz.

Introduction

Recent successes with the chemical vapour deposition of diamond films and doping of natural diamond by ion implantation have brought diamond microelectronics closer to practical realization. To achieve efficient implantation doping for devices, complete recovery and/or epitaxial regrowth of the radiation damaged layers must be realized. This is an interesting problem due to the inherent instability of the diamond phase at normal temperatures and pressures. Unfortunately, the diffusion of vacancies and interstitials as well as the character of various defects in diamond which relate to recovery and regrowth are not well understood.

The Rutherford backscattering/channeling technique provides a quantitative measure of the crystalline quality. Channeling along major crystallographic directions is used to measure implantation damage and annealing. Optical absorption is also effective in determining damage in that several major defect centers¹, as well as the presence of graphite, give strong absorption in the UV-Visible range. PAC is a useful method for determining vacancy trapping configurations.

Low temperature co-implantation of boron atoms with carbon at 77 K followed by rapid heating to high temperatures (~1100 °C) has been used successfully^{2,3} to obtain p-type

layers of low resistivities in insulating type IIa diamond. The samples were implanted at liquid nitrogen temperature in order to prevent diffusion of vacancies and interstitials produced during irradiation. Using this method, the creation of vacancy clusters and lattice dislocations was curtailed⁴. The results of a study of the residual defects in ion implanted and annealed diamonds by using the above mentioned techniques are presented here.

Experimental

Samples used for this study were <100> type Ia and type IIa diamonds. Some samples were re-used after removal of the implanted layers by reactive ion etching with oxygen⁵. All the samples had minimum yields less than 5% before implantation. The minimum yields increased as the samples went thorough a cycle of implantation, RBS analysis and reactive ion etching.

The RBS/Channeling measurements were performed using 2MeV He ions from a 2.5 MV Van de Graaff accelerator at UNC Chapel Hill. The back scattered particles were analyzed with a surface barrier detector mounted at 120° to the incoming beam. The channeling experiments were done with the help of a computer controlled motorized goniometer. The ion implantations were performed in a non-channeling direction at 77 K or 293 K. Some of the samples were rapid thermally annealed to 1100 °C under flowing argon after ion implantation and the others were brought to room temperature and then isochronally annealed in a vacuum furnace (2×10^{-6} torr) up to 1200 °C. Optical absorption measurements were done using a Perkin-Elmer Lambda-9 Spectrophotometer. The channeling measurements as well as optical absorption measurements were done after each anneal. The PAC measurements were performed at the University of Konstanz.

Results and analysis

The results of RBS/Channeling measurements performed on a type IIa diamond sample implanted with 200 keV carbon and 120 keV boron ions are presented in figure 1. The <100> aligned spectrum of the as implanted sample showed a subsurface damage peak, indicating a heavily damaged buried layer about 220 nm below the surface. It is significant that the RBS yield of the damaged layer almost reached the random level. In a parallel study⁶, it was observed that for type Ia diamond samples implanted to a dose of $1.25 \times 10^{15}/\text{cm}^2$ carbon ions, the RBS yield of the damaged layer was well below the random level, whereas for a sample implanted with carbon ions to a dose of $3 \times 10^{15}/\text{cm}^2$, the RBS yield reached the random level and the damaged layer extended all the way to the surface.

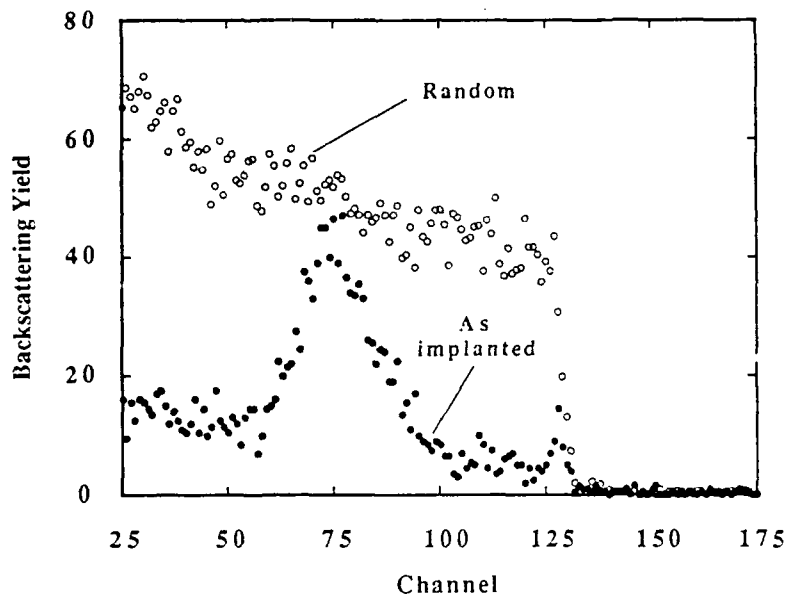
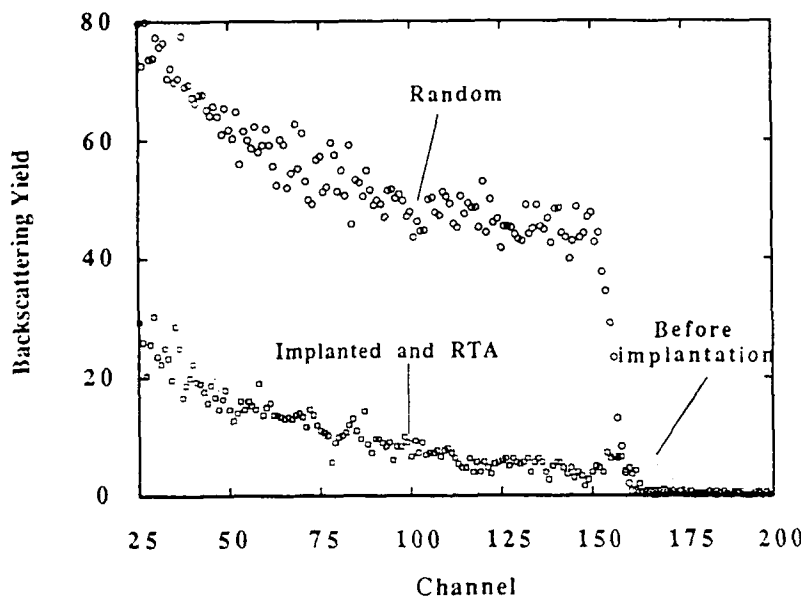


Figure 1 RBS/Channeling spectra of type IIa diamond implanted with 200 keV carbon to a fluence of $2 \times 10^{15}/\text{cm}^2$ and 120 keV boron to $2 \times 10^{13}/\text{cm}^2$ at 77 K. The samples were analyzed at room temperature.

Figure 2 shows results obtained from a type Ia diamond sample implanted with 150 keV carbon and 90 keV boron ions to a dose of $1 \times 10^{15}/\text{cm}^2$ each. It shows that after RTA at 1100 °C for 2 minutes, the radiation damage was completely annealed. This suggests that the diamond structure of the damaged layers was retained after implantation and the defects were essentially point defects and defect clusters. After heating up to 1100 °C, the diamond structure did not collapse and both interstitials and vacancies were mobile and quickly combined to heal the damage. The optical examination as well as optical absorption measurements did not indicate the presence of graphite in the implanted region. This was unlike the case when a sample implanted with 1×10^{15} carbon and 3×10^{15} boron ions per cm^2 turned completely black (due to graphite formation) upon furnace annealing at 1400 °C. Therefore, it can be concluded that a total dose of $2 \times 10^{15}/\text{cm}^2$ in this case is below the critical dose for amorphization, and for graphitization upon subsequent annealing.

In the case of a sample implanted with carbon to a dose of $3 \times 10^{15}/\text{cm}^2$, after RTA at 1100 °C for two minutes the RBS yield in the aligned spectrum was still very high. It was suggested⁶ that this could be due to polycrystalline growth in the amorphous region due to nucleation at high temperature. After subjecting a similar sample to furnace annealing at

Figure 2 RBS/Channeling spectra of type Ia diamond implanted at 77 K with 150 keV carbon and 90 keV boron ions to a dose of $1 \times 10^{15}/\text{cm}^2$ each. The samples were then rapidly heated to 1100 °C for 2 minutes.



500 °C, a small amount of epitaxial growth was observed. However, after annealing at 900 °C for one hour, almost complete epitaxial regrowth occurred from the crystal-amorphous interface all the way to about 53 nm below the surface. The surface layer of about 53 nm thick became graphite which could be scratched off and was etched off in chromic acid, leaving behind a completely transparent sample again. The surface layer presumably acts as a blocking layer which creates pressure to prevent the transformation of the amorphous diamond region to graphite during the annealing process.

The influence of deep implantation on the annealing of damage in natural type IIa diamond was studied using optical absorption. Samples were implanted with 5 MeV C ions at the University of Western Ontario to fluences of 10^{15} to 10^{16} cm^{-2} , and then annealed in vacuum up to 900 °C. In the near edge and visible wavelength range, considerable absorption was caused by the implantation damage (Fig.3), as is usually observed. The unusual feature of the deep implantations was that the high fluence of 10^{16} cm^{-2} did not graphitize the diamond, and that considerable recovery of the absorption in the range 220-900 nm occurred during annealing up to 900 °C even for this high fluence. This result demonstrates that the constraining influence of the overlying good diamond layer for deep implants promoted the regrowth of damaged diamond without graphitization.

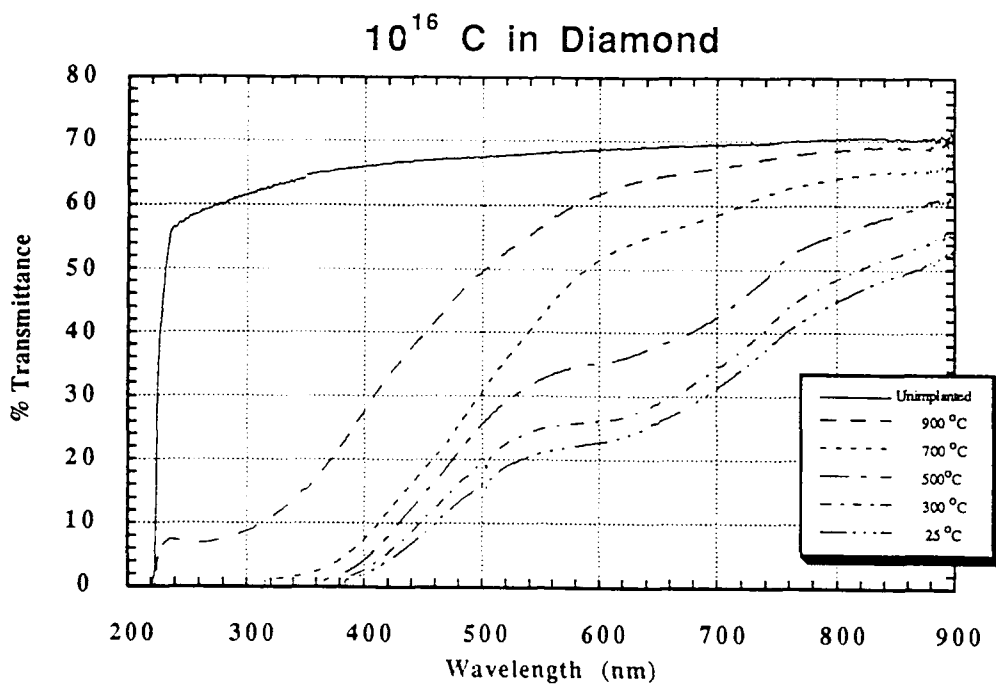


Figure 3 Optical absorption spectrum of a type IIa diamond implanted with C ions to 1×10^{16} per cm^2 at 5 MeV and annealed at different temperatures.

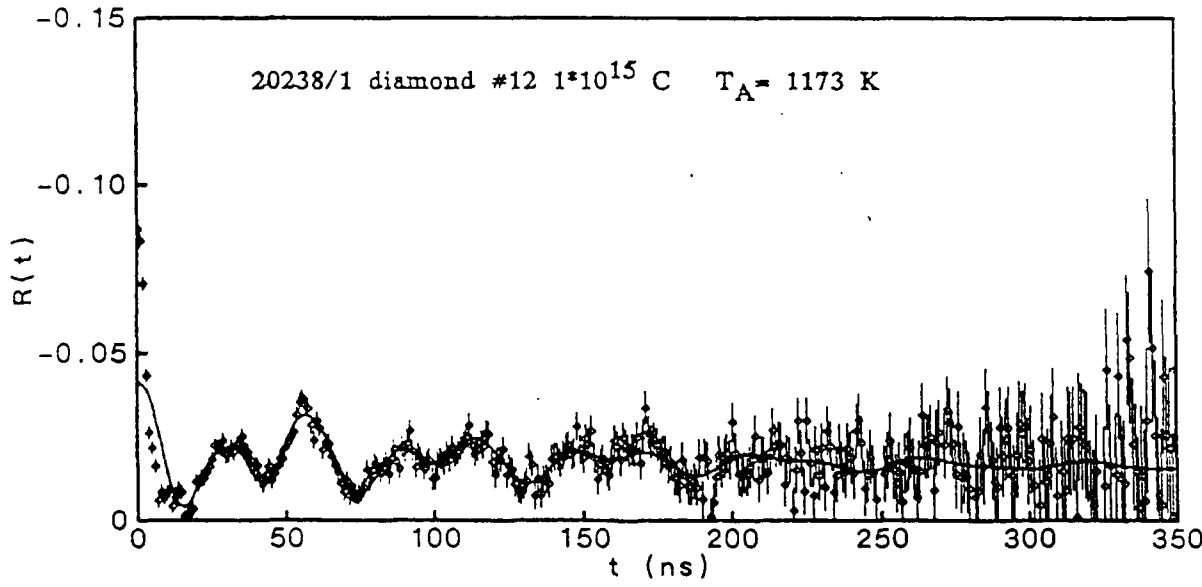


Figure 4 PAC spectrum at 293 K for a type IIa diamond implanted with 10^{15} C ions/ cm^2 at 70 keV and $\sim 10^{12}$ In ions/ cm^2 at 350 keV, followed by a 30 minute anneal at 900 °C in vacuum.

Perturbed angular correlation (PAC) measurements were used to determine the lattice sites of implanted In in natural type IIa diamonds. The samples were co-implanted at 293 K with 70 keV C ions to a fluence of 10^{15} or $2 \times 10^{15} \text{ cm}^{-2}$, and with 350 keV In ions to a small fluence of about 10^{12} cm^{-2} . After implantation, the samples appeared slightly darker in color, and the In atom sites were not distinguishable by PAC because of the radiation damage. After annealing above 1000 K, a considerable fraction of the In atoms occupied well-defined non-cubic symmetry sites, characterized by an electric field gradient with its major component along $\langle 111 \rangle$ and a frequency of 116 MHz. A typical PAC spectrum is shown in Fig. 4, showing 15% of In atoms in those sites. The simplest defect consistent with this site is an In-vacancy pair, with the In atom and vacancy occupying adjacent lattice sites. Thus the vacancy stabilizes the substitutional lattice position of the In atom.

Conclusions

RBS/Channeling measurements showed that for diamond samples implanted with a fluence $\leq 2 \times 10^{15} / \text{cm}^2$ carbon ions at 200 keV, or an equivalent fluence of C plus B ions, the aligned spectrum yield after implantation and annealing coincided with the one before implantation. This is significant due to the fact that by using this methodology, we not only avoided graphitizing the implanted layers, but also regained the diamond crystal structure of the implanted layers. For implantations above this critical dose, unlike the case of shallow implants⁶ where for a sample implanted with $3 \times 10^{15} \text{ C ions/cm}^2$, the 50 nm thick layer at the surface turned into graphite upon furnace annealing, in the case of deep implants, no graphite was observed for samples implanted up to a much higher dose of $1 \times 10^{16} \text{ ions/cm}^2$. This suggests that even for highly damaged layers, graphite formation is prevented by deep implantations. Specific defects (probably In-vacancy pairs) were identified by PAC in diamond; they could provide a powerful method to study other defect interactions and the mobilities of vacancies and self-interstitials in diamond.

This work is supported by the Office of Naval Research contract N00014-87-K-0243.

References

1. J. Walker, Rep. Prog. Phys. **42**, (1979) 1605.
2. G.S. Sandhu, M.L. Swanson and W.K. Chu, Appl. Phys. Lett. **55**, (1989) 1397.
3. J.F. Prins, Nucl. Instr. Meth. **B35**, (1988) 484.
4. J.F. Prins, Phys. Rev. **B38**, (1988) 5576.
5. G.S. Sandhu and W.K. Chu, Appl. Phys. Lett. **55**, (1989) 437.
6. B. Liu, G.S. Sandhu, M.L. Swanson and W.K. Chu, Nucl. Instr. Meth., 1989
(Accepted for publication).

ANNEALING OF IMPLANTATION DAMAGE IN SINGLE CRYSTAL DIAMOND

JOHN D. HUNN, M.L. SWANSON, E.A. HILL, N.R. PARIKH

Dept. of Phys. & Astr., University of North Carolina, Chapel Hill, NC 27599-3255, USA

G. HUDSON

Research Triangle Institute, Box 12194 RTP, NC 27709-2194, USA

ABSTRACT

Thermal annealing of implantation damage in natural single crystal diamond was studied as a function of C^+ dose and annealing temperature. Rutherford backscattering/channelling was employed to measure the amount of damage in the sample. Damage profiles were found to correspond well with simulated vacancy/interstitial pair profiles caused by implantation. The maximum damage density and the minimum anneal temperature for recovery of damage after implantation were determined.

INTRODUCTION

Because of the low diffusivity of most elements in diamond at temperatures below 2000°C , ion implantation is a logical method to introduce electrically active elements into diamond crystals. However, success in implantation doping has been limited not only by the low solubility of most elements, but also by difficulty in annealing out the implantation damage [1-6].

Previous studies of room temperature implantation damage in natural diamond showed that low ion doses produced damage, as observed by ion channeling or optical absorption, that could be almost completely annealed [4-9]. This was true for implantation with both low mass ions like C^+ and high mass ions like Sb^+ . It was inferred from optical absorption and electron paramagnetic resonance studies of irradiated diamond [10-13] that some of the primary defects were vacancies and vacancy clusters (GR1 optical absorption centers). Although many of these defects annealed out in the temperature range 500 - 700°C , some defects, perhaps in the form of larger clusters, persisted even after annealing to 1200°C . Such clusters provide compensating centers in the form of deep donors, thereby reducing the effectiveness of the implantation doping.

Above a certain critical dose, diamond is randomized by ion implantation, as measured by ion channeling. The critical dose was estimated [7,8] to be $3E15 C^+/\text{cm}^2$ at 200 keV and 77 K , and $2E14 Sb^+/\text{cm}^2$ at 350 keV and 300 K . Depending on the ion dose, temperature and depth of implantation, this randomized or amorphous layer may be buried, or may extend to the crystal surface. On annealing, previous results [7] showed that partial recovery of the buried amorphous layer occurred, but that graphitization of the continuous layer occurred. In contrast, our recent results [8,9] show that an apparent epitaxial regrowth of the continuous randomized layer took place during vacuum annealing at 900°C (leaving however, a thin graphite layer on the surface). At higher ion doses, diamond graphitizes spontaneously during implantation [7,14]; subsequent annealing is not required.

In the present experiments, we have used ion channeling to determine the maximum dose of C^+ implantation that permits complete recovery of the implantation damage in natural diamond. We have also studied the optimum annealing conditions for this recovery. In addition, we have investigated the possibility that one or more different phases of diamond may be created by implantation. If a randomized phase of diamond were created, similar to the amorphous phase produced by implantation in Si and Ge, a possible means for removal of implantation damage via epitaxial regrowth could be achieved for

diamond. We have observed that below a critical ion dose, the damaged diamond recovers completely, but above that dose, a "green phase" of diamond appears.

EXPERIMENTAL

Samples were natural single crystal diamonds cut and polished with $<100>$ and $<110>$ surface orientations. Diamonds of both type I-A (containing nitrogen impurity) and type II-a (essentially impurity free) were studied. Most samples were found to possess good single crystal structure as measured by x-ray diffraction and RBS/channelling. Samples were cleaned in boiling chromic acid to remove graphite and foreign matter from all surfaces.

All diamonds were implanted with C^{12} ions in order to create damage without introducing impurities. The samples were implanted at 77 K in order to prevent diffusion of vacancies and interstitial atoms during implantation. We have observed that room temperature implantation produces a broader damage region than equivalent implantation done at 77 K. Implantation was done at energies from 35 to 200 keV and with doses ranging from $5\text{E}14$ to $4\text{E}15 \text{ C}/\text{cm}^2$. The dose rate was kept at $8.7\text{E}11 \text{ ions}/\text{cm}^2\text{s}$. The implantation depth ranged from 0 to 3000 Å below the surface of the 0.25 mm thick crystals.

RBS/channelling was used to measure the depth and degree of damage in the crystal. 2 MeV He^+ ions incident along the $<100>$ or $<110>$ crystal directions varied in backscattering yield from $X_{\min}=0.05$ for undamaged regions to $X_{\min}=1$ for heavily damaged layers (where $X_{\min}=1$ for ions incident in a non-channelling direction). Backscattered ions were detected at 120° to the incoming beam. The majority of damage created by the analyzing beam resides several micrometers below the surface. He^+ irradiation was kept at a minimum and there was no observed damage caused by the analyzing beam.

Three different types of thermal annealing were used to remove implantation damage. Some diamonds were heated in a quartz boat in a conventional tube furnace with a vacuum of less than 10^{-5} Torr. Other samples were annealed in contact with a sapphire crystal heated under a tungsten element in a chamber with vacuum less than 10^{-8} Torr. The third set of diamonds were subjected to rapid thermal annealing (RTA) of 200°C/sec in an argon atmosphere. All three techniques allowed for anneal temperatures up to 1000°C .

RESULTS AND DISCUSSION

Consider carbon ions with an energy of 200 keV implanted in a non-channelling direction into a diamond single crystal. Implanted carbon ions come to rest in a skewed gaussian depth distribution 2000-3000 Å below the surface. Approximately 100 vacancy and interstitial pairs are created by each ion; these are also distributed with a skewed gaussian profile slightly shallower than the implanted ions. The original crystal channels are blocked by interstitial ions and by lattice distortions due to the vacancies; thus the interstitial and vacancy distributions appear as peaks in the channelled RBS spectra. As interstitial/vacancy recombination and/or diffusion occurs the original crystal lattice is restored and the RBS/channelling yield returns to the virgin level. Figure 1 shows the RBS/channelling from a sample implanted with $3\text{E}15 \text{ C}/\text{cm}^2$ at 200 keV. In this sample, a small amount of damage is evident at the surface. The dechannelling increases with depth as the damage density increases and at some point the original lattice is distorted to such a degree that no channelling occurs. Below this heavily damaged region, where the implantation damage does not extend, channelling is again apparent.

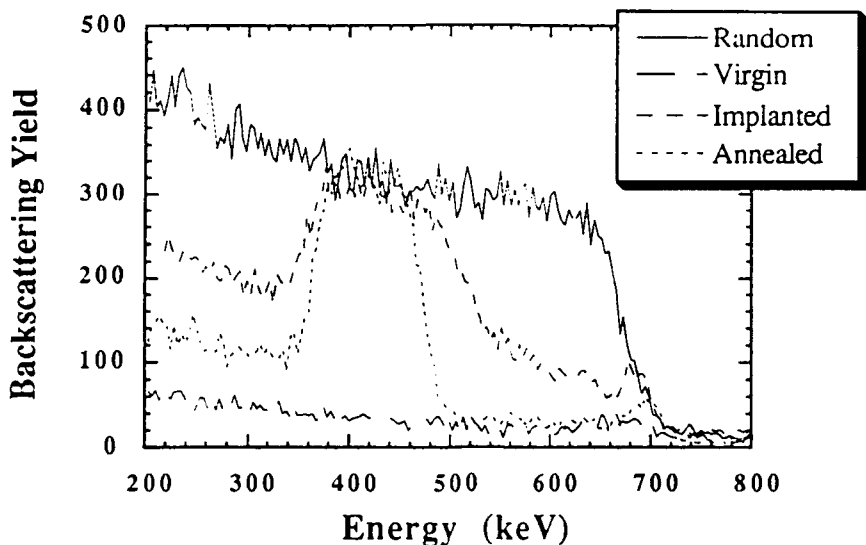


Figure 1: RBS/channelling of diamond implanted with $3E15 C^+/cm^2$ at 200 keV and annealed at $950^\circ C$ for 30 min.

Figure 1 shows the end result of a series of thermal anneals culminating with an anneal at $950^\circ C$ for 30 min. Three distinct regions are apparent in the annealed spectrum. The near surface region shows a complete restoration of the original channelling quality of the crystal. At the back edge of the damaged layer, we also observe a reduction in dechannelling. Dispersion of the incident beam as it passes through the heavily damaged center layer explains why this region does not channel to the virgin level; this is not an effect of damage at this level. The center layer, where the damage density was the greatest, shows no regrowth of the original crystal structure. The sharp drop from the random to the virgin level on either side of this layer suggests a well defined cut-off for the degree of damage from which the original crystal structure can be recovered by thermal annealing.

A region similar to the randomized layer in figure 1 was observed in many samples. In each case, there was a clear demarcation between this layer and the adjacent recrystallized layers. In some cases this region extended all the way to the surface of the sample. After implantation, all the diamonds were varying shades of brown. In samples where the entire implanted region recovered its original virgin channelling yield the samples become very light brown or clear. In annealed samples where the damaged layer did not regrow there was a dramatic change from brown to a striking golden green when viewed from the implanted side and dark reddish brown from the back. Although the original crystal lattice is not restored in this region, this color shift suggests a change from a randomly distributed layer of vacancy/interstitial pairs to a possibly ordered alternate structure. This "green phase" is stable at least to $1100^\circ C$ (limit of our furnace) and is formed by slow heating to $800^\circ C$ as well as RTA to $1000^\circ C$. Wider damaged layers appeared to be deeper green than narrow layers. Raman analysis was performed on a sample with a green layer that transmitted less than 5% at the analyzing wavelength of 514.5 nm. The diamond material in the 1500 \AA layer above the "green phase" gave the expected 1332 nm shift. No other Raman lines were observed including those known to exist for amorphous carbon and graphite.

Figure 2 shows further implantation of the sample in figure 1. Two implantations, 50 keV and 100 keV, left damaged regions in the regrown surface layer of the crystal. After a single 30 minute anneal at $950^\circ C$ complete restoration of the crystal channels is again obtained. In figure 3, another sample is implanted at 50 keV and 100 keV with slightly higher dose. A $950^\circ C$ anneal for 30

minutes resulted in complete recovery of the 100 keV implant damage but only partial recovery in the 50 keV implanted region with the formation of the stable "green phase" in the center of the region where the damage is greatest. With this result and with data from an implantation simulation program (TRIM89 [15]), a maximum damage density for recovery of implantation damage can be estimated.

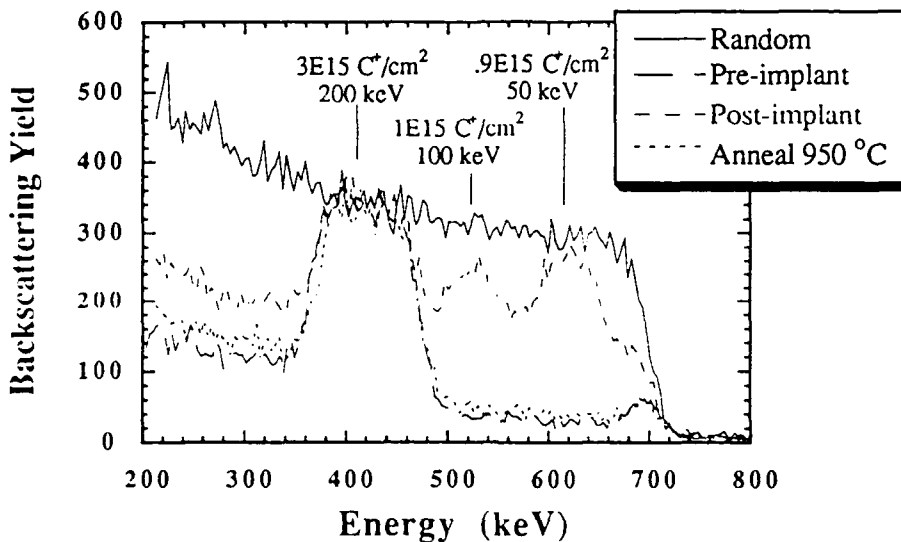


Figure 2: RBS/channelling of diamond implanted at three different energies and annealed at 950°C for 30 min.

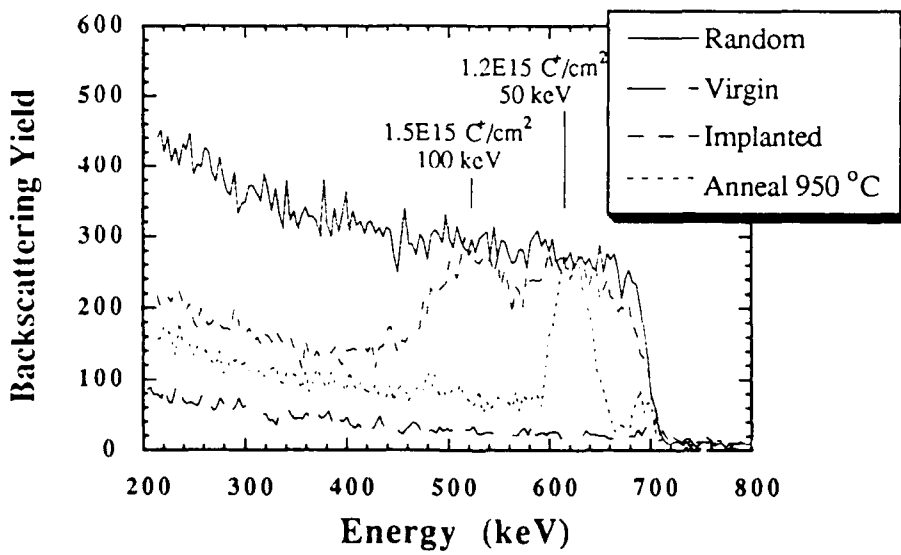


Figure 3: RBS/channelling of diamond implanted at two different energies and annealed at 950°C for 30 min.

Figure 4 shows the simulated vacancies/nm³ for the implantation energies and doses used on the sample in figure 3. We see by overlaying the spectra from figure 3 that the simulation gives a good prediction of the damage distributions observed for these implants. We also see that for a vacancy density greater than approximately 12 vac/nm³ recovery of the crystal lattice does not occur and the "green phase" is formed.

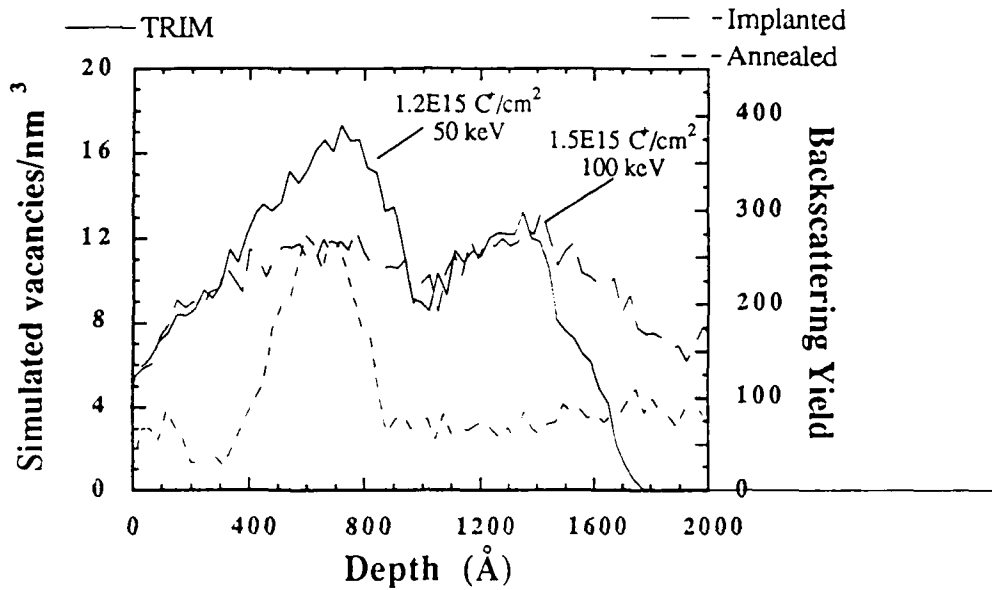


Figure 4: Overlay of simulated vacancy density profile with RBS/channelling profile for a diamond implanted with $1.2\text{E}15 \text{ C}/\text{cm}^2$ at 50 keV and $1.5\text{E}15 \text{ C}/\text{cm}^2$ at 100 keV which is subsequently annealed at 950°C for 30 min.

A sample was implanted with $1.5\text{E}15 \text{ C}/\text{cm}^2$ at 100 keV. From the previous figure we know that this dose does not produce the "green phase". RBS/channelling showed a damage profile that reached the random level at its apex. This sample was subjected to five isothermal anneals the results of which are shown in figure 5. The amount of damage in the crystal after each anneal step was taken as the area under the channelled curve. As the amount of dechannelling in the sample is reduced, this area approaches zero for the virgin sample. The order of annealing proceeds from left to right on the horizontal axis. The graph plots the amount of damage as calculated by RBS/channelling after each anneal. The line is drawn as a guide for the eye. The set of curves illustrates that at each anneal temperature we observed a saturation of the amount of channelling recovery obtained. This saturation suggests some mechanism, possibly related to the size of the vacancy clusters, that is dependent on the temperature of the sample. Most of the peripheral damage in the sample was annealed out at low temperature. This was observed for several samples with noticeable recovery as low as 450°C . The large decrease in damage observed at 800°C corresponds to that temperature where the "green phase" was formed in other samples. After 80 sec at 900°C most of the channelling in the sample was recovered.

Figure 6 shows an isothermal anneal on a sample implanted under the same conditions as that in figure 5. At 900°C we observed rapid recovery of the crystal channels after just 5 seconds. After 80 sec at 900°C almost no dechannelling remained. Samples annealed under vacuum for longer periods showed no better recovery than those annealed for several minutes. The rate at which samples were brought to the anneal temperature showed no effect on the regrowth.

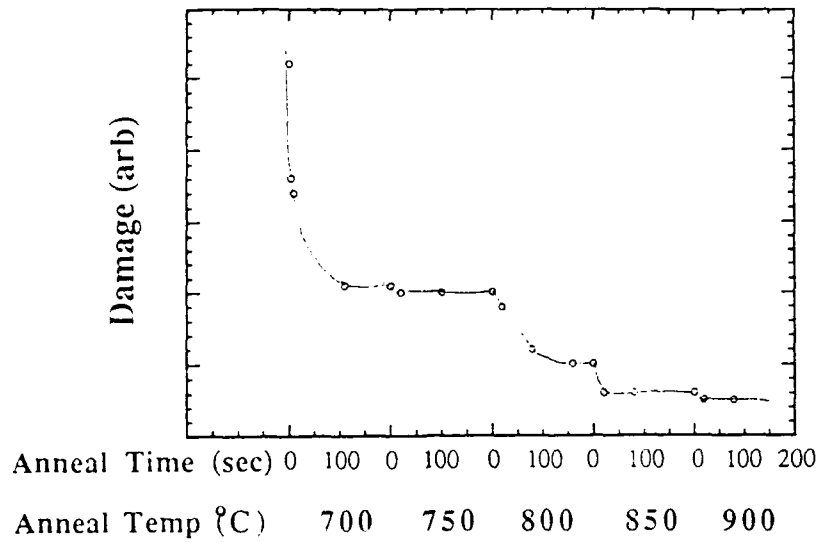


Figure 5: Set of five isothermal anneals on diamond implanted with $1.5E15 C^+/cm^2$ at 100 keV. Damage is plotted in arbitrary units as the area under the RBS/channelling curve referenced to the virgin yield. Anneal times range from 0 to 200 sec for each temperature.

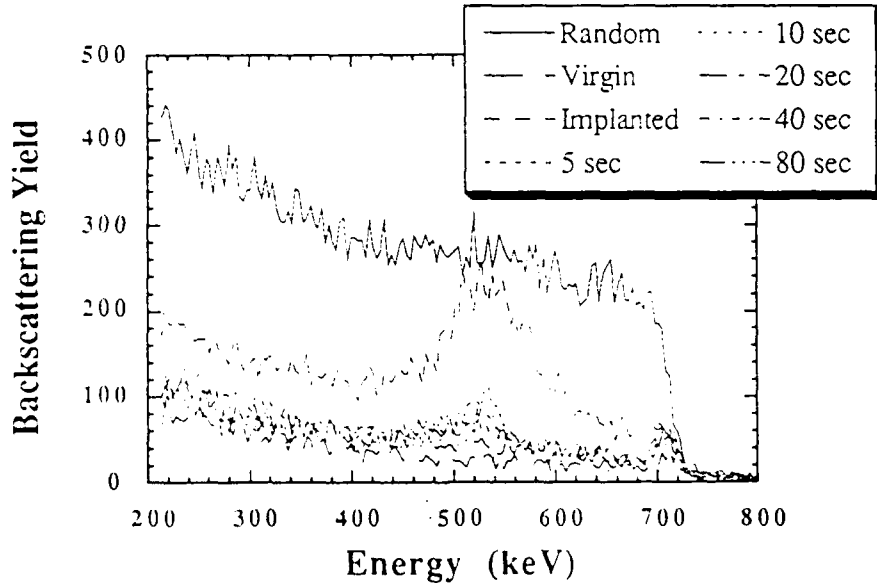


Figure 6: RBS/channelling of diamond implanted with $1.5E15 C^+/cm^2$ at 100 keV and subjected to RTA at 900°C.

CONCLUSION

We have found that the maximum amount of implantation damage from which virgin crystal channeling can be recovered, by thermal annealing up to 1000°C, is approximately equivalent to that caused by a dose of $1.5E15 C^+/cm^2$ at 100 keV. At higher damage densities we observed the formation of a stable region earmarked by a bright green color under reflection, and characterized by a lack of channeling. A temperature dependent mechanism for vacancy/interstitial recombination and/or diffusion was apparent in the anneal studies performed.

An anneal temperature of 900°C was necessary for total recovery of the damage preventing ion channelling. No difference between conventional furnace and rapid thermal annealing was observed. In cases where dopant activation is a concern, RTA is probably preferable.

This work was supported by the Office of Naval Research contract #N00014-87-K-0243 and by Kobe Development Corporation. Special thanks to Barbara Neptune for ion implantation done at the Microelectronics center of North Carolina, Steve Bozeman and Trevor Humphreys for Raman analysis, and J.B. Posthill, R. Rudder and J. Prins for valuable insight.

REFERENCES

1. G. Braunstein and R. Kalish, *J. Appl. Phys.* 54, 2106 (1983).
2. V.S. Vavilov, *Radiat. Eff.* 37, 229 (1978).
3. J.F. Prins, *Phys. Rev. B* 38, 5576 (1988).
4. G.S. Sandhu, W.K. Chu, M.L. Swanson and J.F. Prins, *SPIE Proc.* 969, 37 (1989).
5. G.S. Sandhu, M.L. Swanson and W.K. Chu, *MRS Symp. Proc.* 128, 707 (1989); *Appl. Phys. Lett.* 55, 1397 (1989).
6. G.S. Sandhu, C.T. Kao, M.L. Swanson and W.K. Chu, *MRS Symp. Proc.* 162 (1990) .
7. G. Braunstein, A. Talmi, R. Kalish, T. Bernstein and R. Beserman, *Radiat. Eff.* 48, 138 (1980).
8. B. Liu, G.S. Sandhu, N.R. Parikh, M.L. Swanson and W.K. Chu, *Nucl. Instr. Meth. B* 45, 420 (1990).
9. G.S. Sandhu, B. Liu, N.R. Parikh, J.D. Hunn, M.L. Swanson, Th. Wichert, M. Deicher, H. Skudlik, W.N. Lennard and I.V. Mitchell, *MRS Symp. Proc.* 162 (1990).
10. C.D. Clark and E.W.J. Mitchell, *Radiat. Eff.* 2, 219 (1971).
11. J. Walker, *Rep. Progr. Phys.* 42, 1605 (1979).
12. J.E.W. Lowther, *J. Phys. Chem. Solids* 45, 127 (1984).
13. J.N. Lomer and A.M.A. Wild, *Radiat. Eff.* 17, 37 (1973).
14. R. Kalish, T. Bernstein, B. Shapiro and A. Talmi, *Radiat. Eff.* 52, 153 (1980).
15. J.F. Ziegler, *Transport of Ions in Matter (TRIM)*, IBM corp software (1989).

DOPING OF DIAMOND BY CO-IMPLANTATION WITH DOPANT ATOMS AND CARBON

G.S. Sandhu, C.T. Kao, M.L. Swanson, Department of Physics and Astronomy, University of North Carolina, Chapel Hill, NC 27599-3255;
W.K. Chu, Texas Center for Superconductivity, University of Houston, TX 77204-5506.

Abstract

We have investigated the challenging problem of doping diamonds, by co-implanting boron, nitrogen or phosphorus together with carbon into natural insulating type IIa diamonds. All the implantations were done at liquid nitrogen temperature and then the samples were rapidly heated to 1100 °C. Unlike the previous attempts to dope diamond by room temperature or high temperature ion implantations, this method is expected to yield a higher doping efficiency for the implanted atoms. We have characterized the implanted diamonds with electrical and electron spin resonance (EPR) measurements. Boron doped samples showed low electrical resistivities and the EPR signal showed a strong dependence on the boron fluence, indicating a high substitutional fraction of boron atoms. The samples in which nitrogen and phosphorus were co-implanted with carbon showed lower resistivities compared with samples implanted with carbon only. Preliminary thermo-emf measurements indicated n-type conduction in these samples.

Introduction

Ion implantation is the most promising technique to dope diamond in a controlled manner. So far, this method has had limited success^{1,2} because it requires finding annealing conditions which will drive the implanted atoms into electrically active sites and restore the diamond crystal structure, tasks which are complicated at high ion doses by the tendency of the damaged diamond to turn into graphite^{3,4}. When the ion dose is low enough to prevent graphitization, very few of the dopant atoms end up in electrically active sites^{1,4}. Low temperature co-implantation of boron atoms with carbon at 77 K followed by rapid thermal annealing (RTA) at 1100 °C has been used successfully⁵ to obtain p-type layers of low resistivities in insulating type IIa diamonds. Photoconductivity measurements of the samples indicated the presence of deep donor centers which could be negatively charged vacancies.

Electron spin resonance studies of impurities as well as various kinds of defects in diamond have been reviewed by Loubser⁶. The EPR of bound nitrogen donors in diamond

was utilized to identify various kinds of nitrogen clusters in type I diamonds⁷⁻¹⁰. Based on their EPR measurements for electron irradiated diamonds at low temperature, Lomer and Wild¹¹ suggested that interstitials in diamond are mobile below room temperature. They further observed EPR spectra¹² produced by vacancy clusters of different sizes after annealing the samples at various temperatures up to 1400 °C.

The n-type doping of diamond is a major problem which has to be surmounted before a variety of practical devices using diamond can be fabricated. Some of the dopant atoms such as phosphorus, nitrogen etc. have been implanted into diamond in the past. However, due to compensation by a large number of residual defects, the resistance of the implanted samples was very high. There is a possibility of achieving better results if one uses the method of low temperature implantation followed by RTA⁵. Preliminary experiments by co-implanting with phosphorus or nitrogen together with carbon at low temperature are presented here.

Experimental

Type IIa natural insulating diamond square plates of dimensions 3x3x0.5 mm were implanted with carbon ions and then with the dopant ions at 77 K. The various implantations are summarized in table I. All the samples were then rapidly heated under flowing Argon from liquid nitrogen temperature to 1100 °C in a Heatpulse RTA furnace. The resistivity of these samples as a function of temperature was measured using a Keithly electrometer. The EPR experiments were performed on a Brucker ER200tt spectrometer which was interfaced to an IBM-compatible personal computer. The temperature of the samples could be maintained at any value from 5K to room temperature with the help of a set of cryogenic units. The diamond plates were glued onto the flat end of a quartz rod with commercially available rubber cement, and inserted into the microwave cavity between the magnet poles of the spectrometer. In general, the EPR spectra for each sample was taken at 20 K, 70 K and 95 K. In some cases, EPR spectra were also taken at different angles at a given temperature. Although the samples were certified to be of <100> orientation perpendicular to the flat surface (in the horizontal plane), the orientation along the vertical z-direction (rotation axis) of the as mounted sample was not known. Consequently, the EPR data as a function of angle could not be used for detailed analysis except for determination of the anisotropy of the EPR center.

Results and analysis

Typical EPR spectra obtained from a set of implanted diamond samples are shown in figure 1. Within the resolution of the spectrometer, the signal consisted of a single line in

Table I. Summary of the process parameters for various Ion Implantations into diamond. See reference 5 for more details.

SAMPLE	IMPLANTED ION	ENERGY (keV)	FLUENCE (atoms/cm ²)
a	C	100	6x10 ¹⁴
followed by	N	110	2x10 ¹⁴
b	C	200	2x10 ¹⁵
followed by	P	300	3x10 ¹⁴
1	C	200	2x10 ¹⁵
2	C	200	2x10 ¹⁵
followed by	B	120	1x10 ¹⁴
3	C	200	2x10 ¹⁵
followed by	B	120	3x10 ¹⁴

all the samples studied. The EPR line height increased with the boron fluence in the implanted samples. The ratio of line heights of samples 3 and 2 was close to 1.6 in the temperature range from 20 K to 90 K. This indicates that the number of EPR centers in the sample was strongly dependent on the boron concentration since the ratio of boron fluence was 3:1 but the total fluence differed only by 9 percent. Therefore, it seems that the boron atoms in the lattice were either directly responsible for producing the EPR signal or indirectly influencing the EPR line intensity by perhaps exchanging charge with the EPR centers.

The width of the EPR line for samples 2 and 3 measured at 70 K and 95 K is plotted as a function of the direction of magnetic field in figure 2. All the samples showed a similar variation in the line width with angle. The variation in the line height with angle did not correlate with the width, suggesting that the EPR line might be a superposition of signals from two different centers. The anisotropy in the line width could at least partially be due to the unresolved hyperfine structure.

EPR of heavily boron doped synthetic diamonds has been reported in the literature¹³. They observed two EPR lines which were described as being due to free and bound holes. These lines were not observed in natural semiconducting diamonds. Ammerlaan¹⁴ has reported EPR spectrum of natural type IIb diamonds. The EPR signal was seen below 2 K and only when stress was applied to the samples. Bell and Leivo¹⁵ reported sharp EPR lines at g=2.003 for several natural semiconducting diamonds in the temperature range 108-

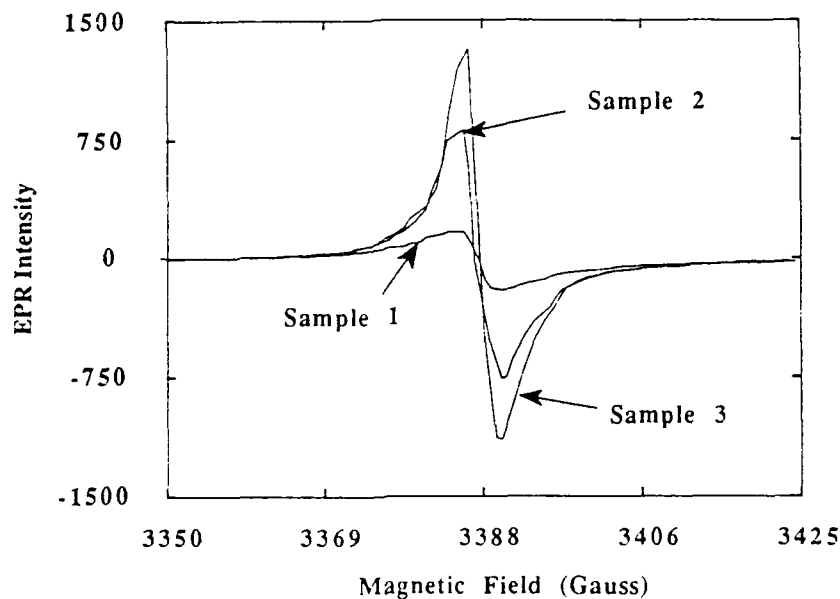


Figure 1 EPR spectra taken at 20 K for three diamond samples 1, 2 and 3 (table I) implanted with 200 keV carbon to 2×10^{15} per cm^2 each and 120 keV boron to 1×10^{14} and 3×10^{14} per cm^2 for samples 2 and 3 respectively. After implantations, all the samples were RTA at 1100 °C for 2 minutes.

370 K under no applied stress. They attributed the sharp line to acceptor centers on the basis that the number of acceptors was comparable to the number of spins measured.

In the present study, the variation of line width with angle suggests that the source of the EPR signal might consist of at least two different types of centers. One of the centers could be a charged vacancy and/or vacancy clusters and the other associated with a free or bound hole. There is presumably enough built-in strain after ion implantation and annealing in these samples to make it possible to detect EPR signal from bound holes as seen by Ammerlaan¹⁴. Bell and Leivo¹⁵ suggested that the EPR signal in their natural semiconducting samples could be associated with acceptor centers in the samples and the unpaired spin may be located at a vacancy or multiple vacancy cluster in the diamond lattice. Therefore, the variation in line intensity with boron fluence can be explained by considering the source of the EPR signal as being boron atoms through free or bound holes and/or charged vacancies which can exchange charge with the boron atoms in the lattice.

Figure 3 shows the plot of resistance versus temperature for samples a and b implanted with nitrogen and phosphorous ions (table I). For comparison, data for sample 1 implanted only with 200 keV carbon to 2×10^{15} per cm^2 are also shown. It is encouraging

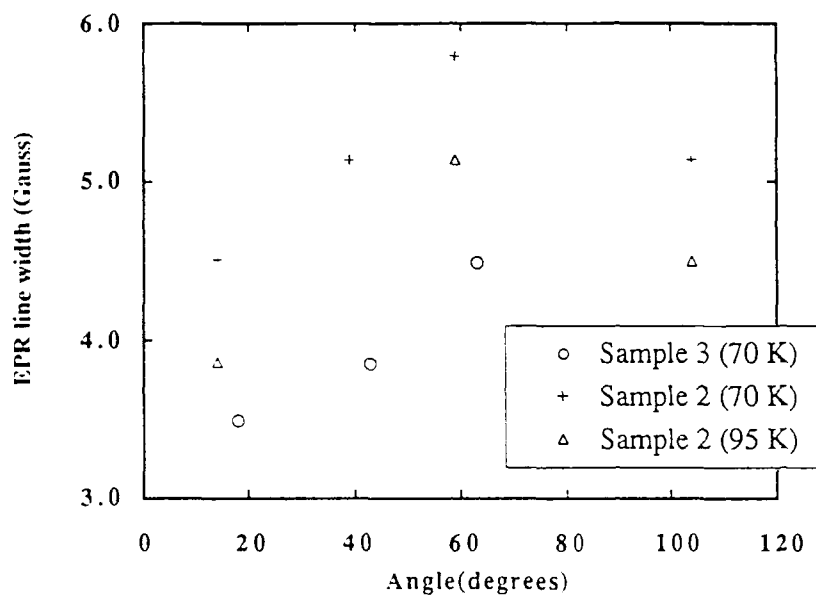


Figure 2 Width of the EPR line at different temperatures for samples 2 and 3 (table I) as a function of the angle.

to note that the resistance of both P and N doped samples was lower than that of the sample doped with C only. Preliminary thermo e.m.f. measurements on the P and N doped samples indicated n-type conduction.

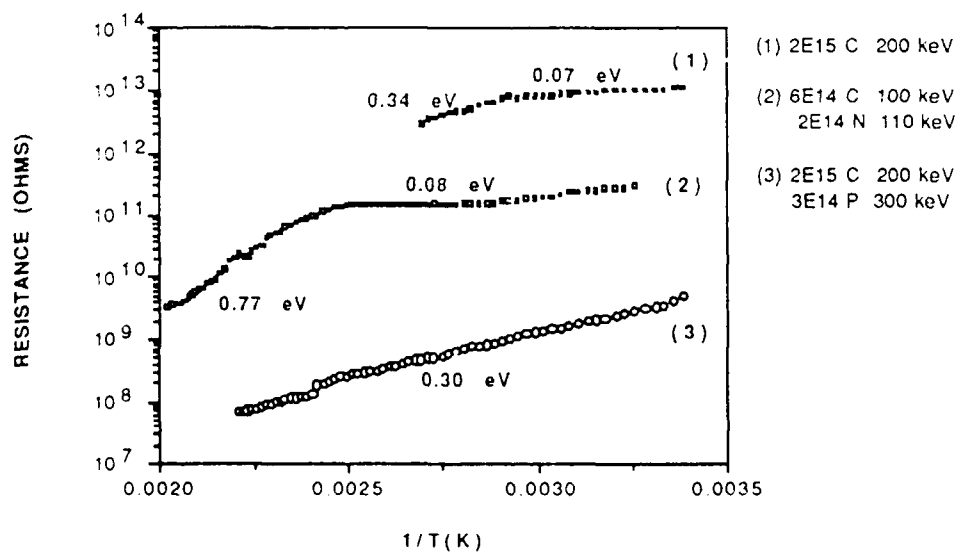


Figure 3 The plot of resistance versus $1/T$ for samples a and b in table I.

The I-V characteristics of the phosphorus implanted sample (same as in figure 3) did not show ohmic characteristics¹⁶. This was unlike the case where a similar curve for a sample implanted with boron showed ohmic behaviour^{5,16}. Since the boron implanted samples were shown to be p-type (Hall measurement), and the contacts in both cases were made using the same method, it seems plausible that in the case of phosphorus the conductivity type of the doped layer is not p-type. The I-V curve could represent back-to-back diode characteristics with a high leakage current.

Conclusions

The intensity of the EPR signal for the diamond samples co-implanted with carbon and boron was found to depend strongly on the boron fluence. This suggested that the boron atoms influenced the EPR signal through charge exchange with the residual defects in the diamond lattice and that the electrical conductivity of these samples was primarily due to the activation of boron atoms. Preliminary results on phosphorus and nitrogen implanted samples showed low resistivities, and there is some evidence that n-type conductivity was achieved.

This work is supported by the Office of Naval Research contract N00014-87-K-0243.

References

1. G. Braunstein and R. Kalish, J. Appl. Phys, **54**, 2106 (1983).
2. V.S. Vavilov, M.S. Gukasyan, M.I. Guseva, and E.A. Konorova, Sov. Phys. Semicond. **6**, 742 (1972).
3. R. Kalish, T. Bernstein, B. Shapiro and A. Talmi, Rad. Eff. **52**, 153 (1980).
4. G. Braunstein, A. Talmi, R. Kalish, T. Bernstein and R. Beserman, Rad. Eff. **48**, 139 (1980).
5. G.S. Sandhu, M.L. Swanson and W.K. Chu, Appl. Phys. Lett. **55**, 1397 (1989) .
6. J.H.N Loubser and J.A. van Wyk, Rep. Prog. Phys. **41**, 1201 (1978) .
7. W.V. Smith, P.P. Sorokin, I.L. Gelles, and G.J. Lasher, Phys. Rev. **115**, (1959) 1546.
8. J.A. van Wyk, J. Phys. C: Solid State Phys. **15**, (1982) L981-L983.
9. J.A. van Wyk and J.H.N. Loubser, J. Phys. C: Solid State Phys. **16**, (1983) 1501.
10. J.H.N. Loubser, J.A. van Wyk and C.M. Wellbourn, J. Phys. C: Solid State Phys. **15**, (1982) 6031.
11. J.N. Lomer and A.M.A. Wild, Phil. Mag. **24**, 272 (1971).
12. J.N. Lomer and A.M.A. Wild, Rad. Eff. **17**, (1973) 37.
13. J.C. Bourgois, P.R. Brosious, Y.M. Kim, J.W. Corbett and R.M. Chrenko, Phil. Mag. **26**, (1972) 1167.
14. C.A.J. Ammerlaan, Inst. Phys. Conf. Ser. No. 59, Oiso Japan (1980).
15. M.D. Bell and W.J. Leivo, J Appl. Phys. **38**(1), (1967) 337.
16. G.S. Sandhu, PhD thesis, University of North Carolina, Chapel Hill NC, 1989.

Ion Implantation Doping of Diamond

Edward Hill, John Hunn, Nalin R. Parikh, and Max L. Swanson

Department of Physics and Astronomy

University of North Carolina, Chapel Hill, NC

Ray Zehr and David Geohegan

Oak Ridge National Laboratory, Oak Ridge, TN

Abstract

We have studied ion implantation as a possible method of doping diamond for semiconducting applications. Diamond samples were implanted with lithium or sodium. Various anneals were performed on the implanted samples. Electrical measurements and Neutron Depth Profiling have been used for the characterization of samples. In addition, two methods of making electrical contact to diamond have been explored.

Motivation and Objective

The chemical, physical, and electrical properties of diamond make it a desirable material for microelectronic device construction. Such devices would be radiation hard and capable of high temperature operation due to the large band gap of diamond, 5.5 eV. High thermal conductivity, chemical inertness, and mechanical strength are also important qualities of diamond. As with silicon, also a group IV element, successful doping of diamond is required to create useful semiconductor devices. Due to difficulties with diffusing impurities into diamond or introducing impurities during crystal growth, ion implantation is a promising alternative method of doping.

P-type semiconduction (i.e. conduction via holes) is caused in some natural diamonds by boron impurities. P-type diamond has also been made by ion implantation of boron into diamond. N-type diamond (i.e. conduction via electrons), however, has proven to be far more difficult to produce yet it is crucial to device construction. Lithium and sodium are likely n-type dopants¹. These atoms are assumed to occupy interstitial sites. A dopant with small atomic radius is more likely to reside at active dopant sites within the dense diamond lattice. Proper annealing may be necessary to remove implantation damage, yet dopant diffusion during the anneal must be considered. In this work we have studied diamonds implanted with lithium or sodium.

Making good electrical contact to an implanted layer in diamond is a significant technological hurdle. This work uses contacts made by patterned ion implantation damage for conduction to the implanted layer. LASER induced damage, which may be useful for making contacts, was also explored. Stable, ohmic electrical contacts are necessary for proper analysis of dopants.

Experimental Procedure and Results

Single crystal (100), type II-A, 3mm x 3mm x 0.25mm diamond windows were used as samples. ²³Na and ⁶Li doses of 1×10^{15} ion/cm², with energies of 100 keV and 35 keV respectively, were implanted at 77 K at ORNL. The implanted layers are roughly 100 nm deep. Using a mask, a B⁺ dose of 3×10^{16} ion/cm² was implanted at 54 keV into the corners of the

sample surface. Tungsten probes, pressed onto the corner regions, served as electrical contacts for measurements.

Electrical measurements and an anneal were performed on the sodium implanted sample. A test of current versus voltage showed that we had ohmic contacts. The resistance versus temperature measurement, prior to the anneal, showed an electrical activation energy of 0.26 eV (see fig. 1). The sample was then annealed for 30 minutes at 950 °C in a vacuum furnace. The resistance versus temperature measurement showed an electrical activation energy of 0.14 eV after the anneal. There was also an overall drop in the sample resistance. These facts imply that some activation of the sodium occurred during the anneal.

The lithium implanted sample was first analyzed by Neutron Depth Profiling (NDP). This method is useful for determining a concentration versus depth profile of certain elements² (see fig. 2). The sample was then annealed for 10 seconds at 1000 °C in an argon atmosphere and again analyzed by NDP. Only a small amount of change was seen in the lithium concentration versus depth profile. This is promising because significant lithium diffusion during the annealing of implantation damage would make this method ineffective. At this point, measurement of resistance versus temperature showed an electrical activation energy of 0.02 eV; this low value of activation energy is associated with variable range hopping conduction due to the implantation damage. A subsequent anneal for 10 minutes at 950 °C increased the sample resistance by a factor of 1000, yet the activation energy changed to 0.22 eV. These facts imply that the implantation damage was healed and perhaps some of the lithium became electrically active.

We have also performed a preliminary study of LASER induced damage in diamond. LASER damage could be a useful substitute for ion implantation damage as a method of making electrical contact to an implanted layer. A diamond sample was exposed to a 1.5 J/cm² pulse of the 193 nm line of a ArF LASER at ORNL. A heavily damaged (i.e. dark) strip across the sample was the result. Resistances across the surface of the strip were a factor of 10 lower than that of an ion implantation contact surface. Based on the surface dimensions and the resistance of the LASER damaged region the depth of the damage is estimated to be 150 nm. This would be a sufficient depth to reach the implanted layers used in this work.

Resistance of Na Implanted Diamond

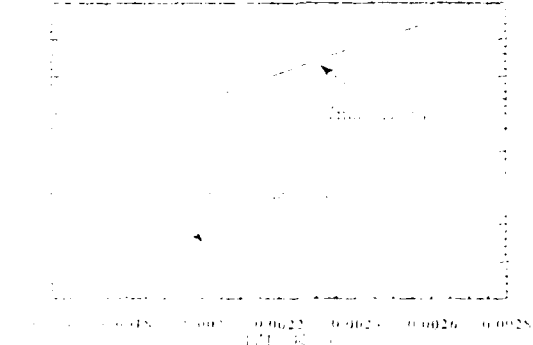


Figure 1- Plot of log of resistance versus inverse temperature for the sodium implanted sample before and after annealing. Activation energies are proportional to the slopes of the lines.

Neutron Depth Profile of Li after anneal

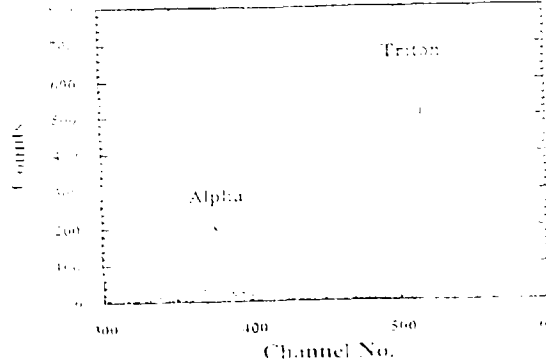


Figure 2- Plot of counts(yield) versus channel number(energy) from the ${}^6\text{Li} + \text{n} \rightarrow {}^4\text{He} + {}^3\text{H}$ nuclear reaction due to thermal neutrons hitting the lithium implanted sample. This gives concentration versus depth data.

Conclusion

In this work we have explored the use of ion implantation as a means to dope diamond. Lithium and sodium implantations were performed and then analyzed by electrical measurements and Neutron Depth Profiling. Changes in electrical activation energies were observed after annealing. NDP results show that there was not significant diffusion of the lithium at the anneal temperature used. It has also been seen that LASER damage is a possible means of making contacts on diamond. Ion implantation doping of diamond is an important step towards technological applications. This research, including a high temperature Hall effect system for obtaining more information about dopants, is an ongoing project at UNC Chapel Hill.

Publication

Experimental results reported in this paper were included in a poster presented by Edward Hill at the 1990 Ion Beam Modification of Materials conference in Knoxville, TN.

Acknowledgements

We would like to express our gratitude to Ray Zuhr of the Oak Ridge National Laboratory Solid State Division for his help with the implantations for this experiment. We would also like to thank David Geohegan at ORNL for performing the ArF LASER work.

References

1. J. Bernholc, S. Kajihara, and A. Antonelli, *Second International Conference on the New Diamond Science and Technology*, Washington, DC (1990).
2. R. G. Downing, R. F. Fleming, J. K. Langland and D. H. Vincent, Nuclear Instruments and Methods in Physics Research 218 (1983) 47-51.

IMPACT OF UNC-CH (PHYSICS)

COLLABORATION ON RTI'S DIAMOND PROGRAM

The collaborative arrangement that exists between the Microelectronics Group in the Department of Physics and Astronomy at UNC-Chapel Hill and the Device Research Department in the Center for Semiconductor Research at the Research Triangle Institute has been a fruitful and productive one. This has been most evidenced by the research that pertains to the SDIO/IST-funded diamond program at RTI. Certain examples follow that illustrate the type of joint work that has directly impacted the diamond program.

I. Homoepitaxial Diamond

A new method of diamond CVD has been pioneered at RTI, which involves only the pyrolysis of a CF_4/F_2 gas mixture¹. The characterization of a homoepitaxial diamond film grown in this manner on type 2B (100) diamond included RBS/channeling studies at UNC-CH (Fig. 1). Axial [100] channeling could not be achieved on this film but planar channeling was observed. As ongoing RBS/channeling studies of several different natural diamond single crystals at UNC-CH showed that it was rare to achieve axial channeling on type 2B diamond single crystals due to a subgrain structure, it was presumed that this subgrain structure propagated into the grown film. The achievement of planar channeling does indeed show that the film is epitaxial.

II. Metal Single Crystal Preparation and Epitaxy

Another part of the RTI effort to achieve heteroepitaxial semiconducting diamond involves the engineering and fabrication of lattice-matching metal substrates. This involves the initial crystal preparation and the subsequent epitaxial growth of Ni, Cu, and Ni-Cu alloys and superlattices⁵ on Ni(100) and Cu(100) single crystals. The optimization of this process has required extensive analytical characterization, which has included RBS/channeling to assess substrate preparation processes and epitaxial film quality. Figures 2-5 shows representative RBS/channeling results. It can be readily seen that the crystal perfection of Ni(100) after Syton polishing (colloidal silica) is far superior to the as-polished Cu(100). As a result of this, RTI has chosen to utilize Ni(100) crystals exclusively. Figures 4 and 5 show results from epitaxial metal films grown by molecular beam epitaxy. As expected, homoepitaxial Ni is of higher crystalline perfection than epitaxial Ni₇₅Cu₂₅. This particular alloy film was grown to lattice-match diamond at a growth temperature of 700°C. Although the surface morphology was excellent for both, it appears that further optimization will be required for high-quality Ni-Cu alloy epitaxial film growth. This work will be presented jointly at the Fall 1989 MRS meeting in Boston, MA².

III ERD for H in Diamond

Figure 6 shows ERD results that compare the hydrogen concentration in two RTI diamond thin films grown on scratched Si(100) by immersion plasma-enhanced CVD. Both samples were grown using a 1% CH₄ in H₂ gas mixture at a pressure of 5 Torr. Sample heating was accomplished inductively by a graphite susceptor and was varied

by altering the height of the sample stage with respect to the rf coils. Sample No. 1 was grown in closer proximity to the coils and hence at a higher temperature than sample No. 2. Sample No. 2 appeared morphologically much smoother than sample No. 1, and sample No. 2 did not have the characteristic 1332 cm^{-1} Raman signature. ERD shows that these results for sample No. 2 are concomitant with a high hydrogen content. The hydrogen concentration for the bona fide diamond film on Si (sample No. 1) is at or below the limit of detectability for the technique.

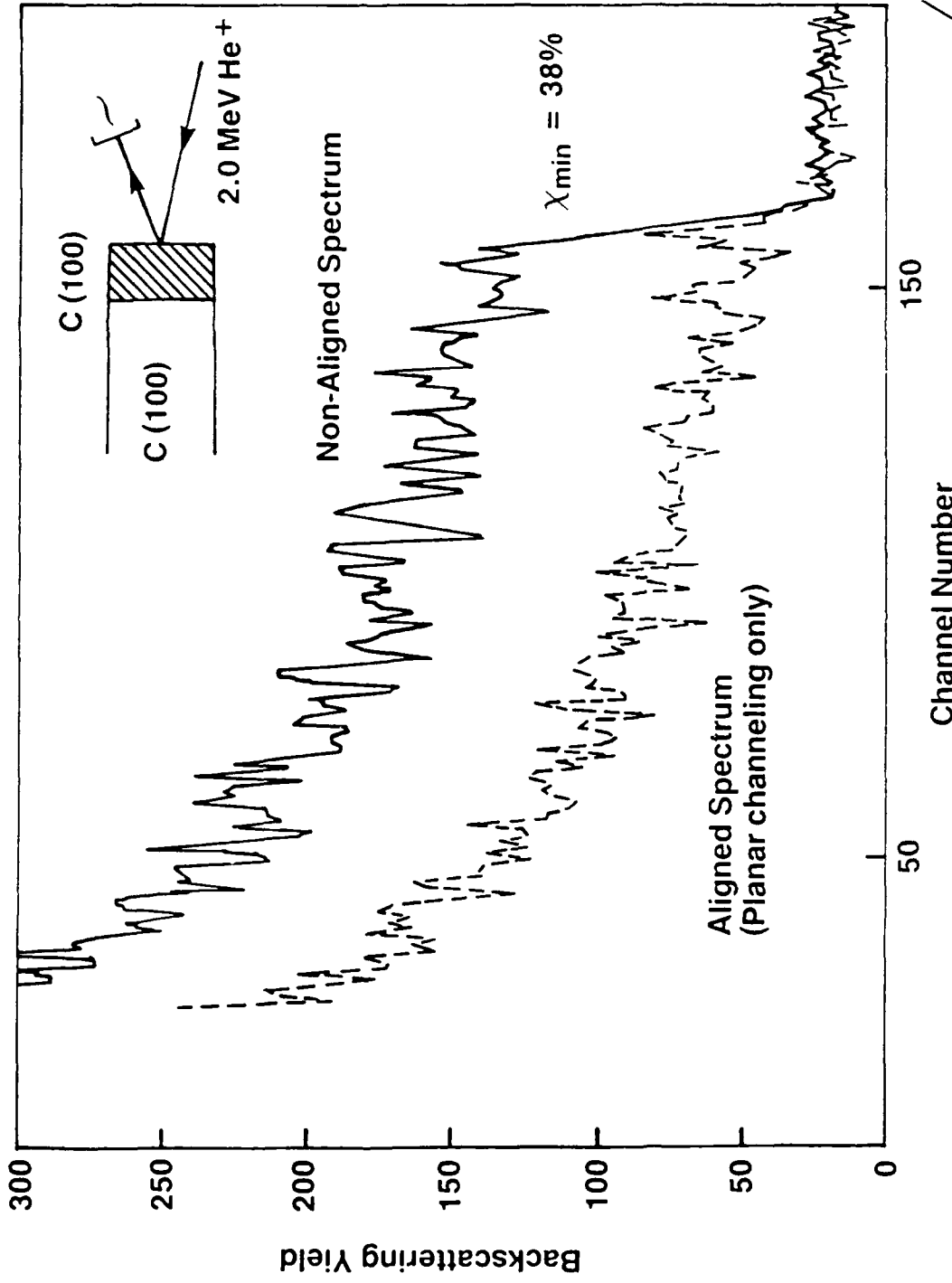
References

1. R.A. Rudder, J.B. Posthill and R.J. Markunas. Electronics Lett., 25, 1220 (1989).
2. R.P. Burns, Y.H Lee, N.R. Parikh, J.B. Posthill, M.J. Mantini, and R.J. Markunas. Fall 1989 MRS meeting, "Layered Structures - Heteroepitaxy, Superlattices, Strain and Metastability", to be presented Nov. 28, 1989, Boston, MA.

J.B. Posthill

16 October 1989

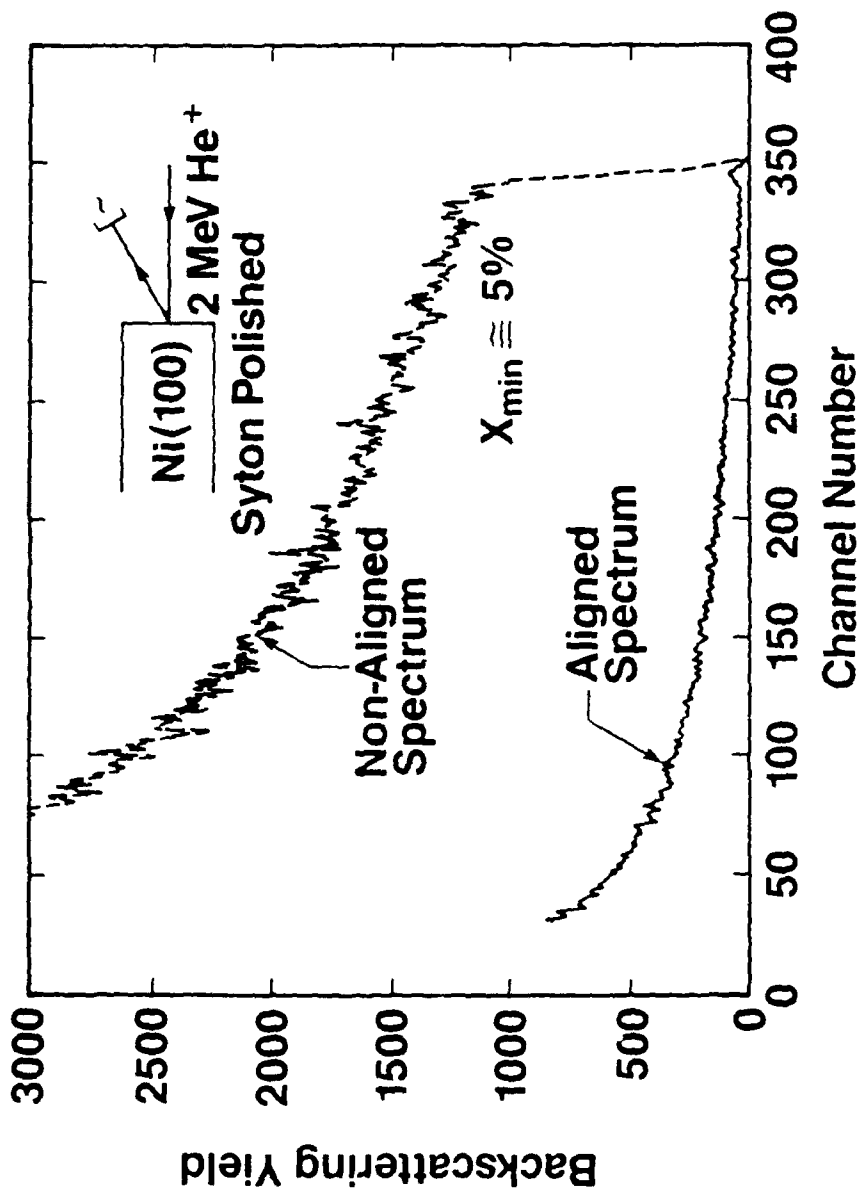
RBS/Channeling Spectra from
PECVD Homoepitaxial Diamond
[C-061989-C (100)]



RTI

Fig. 2

RBS/Channeling from Syton Polished Ni(100)



✓RTI

RBS/Channeling from Syton Polished Cu(100)

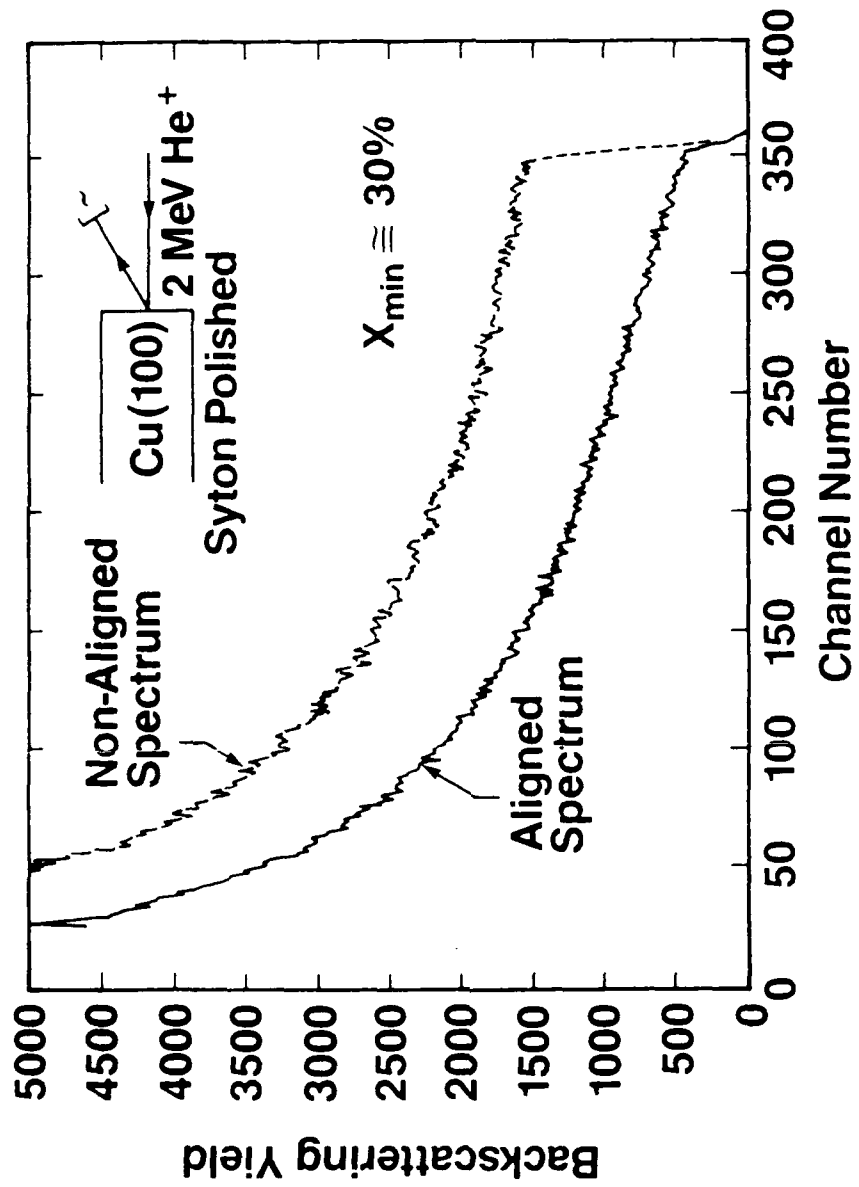
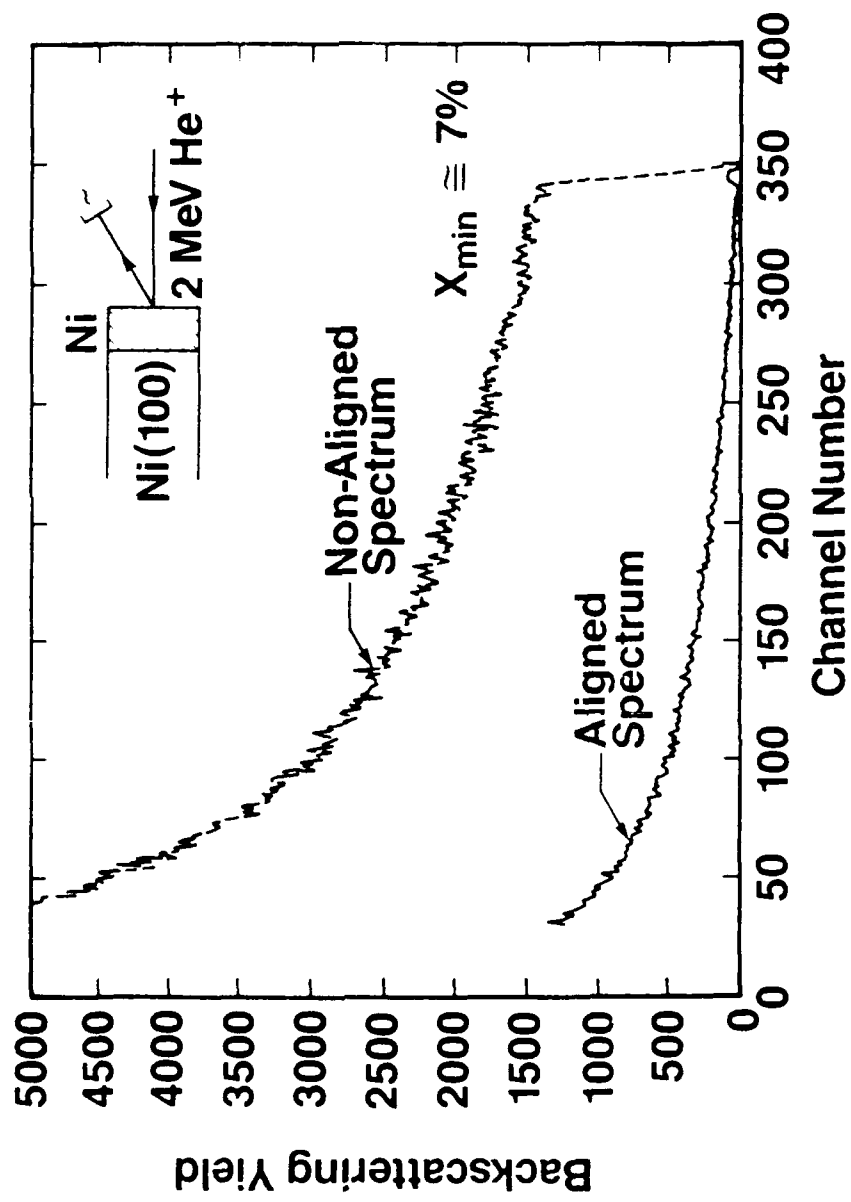


Fig. 4.

RBS/Channeling from 1000 Å Ni/Ni(100)
Grown at 300 °C



RBS/Channeling from 1000 Å 75 Ni-25 Cu/Ni(100)
Grown at 300 °C

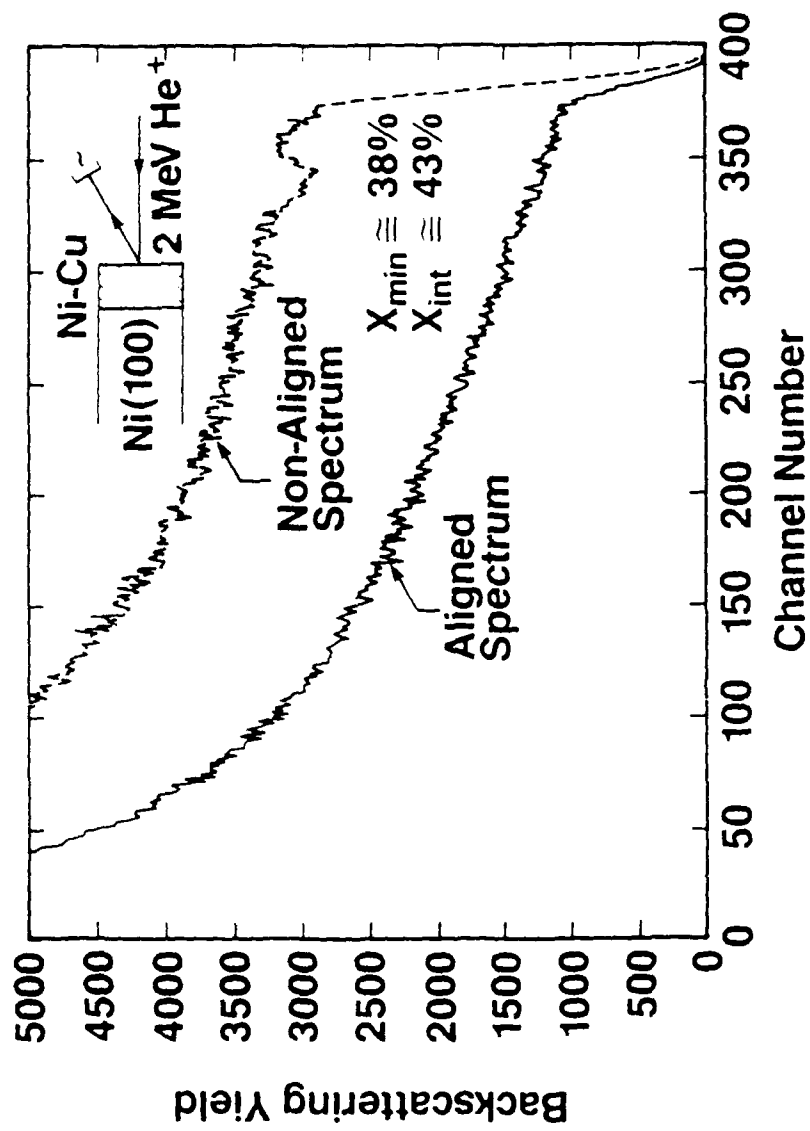


Fig. 5

Fig. 6.

